FABRICATION OF TUNGSTEN CARBIDE NANOPARTICLES BY ELECTROCHEMICAL ETCHING OF TUNGSTEN IONS IMPLANTED SUBSTRATE

Usman Niaz[a*], M. Shahid Rafique[a], Ayesha Jamil[a], Basit Ali[a], M. Bilal Tahir[b]

[a]Laser and Optronics Center, Department of Physics, University of Engineering and Technology, Lahore, Pakistan

[b]Department of Physics, University of Gujrat, Gujrat, Pakistan

ABSTRACT: *Tungsten carbide (W_2C) nanoparticles have been fabricated by electro chemical etching of ion implanted graphite surfaces. Nd: YAG laser (1064nm, 9-14 ns, and 10 mJ) was used to irradiate the tungsten (W) target for the production of laser generated ions, the ions were extracted from the laser induced plasma by the self generated electric field, then the energy of the tungsten ions was measured as 10.368 keV by using Thomson Parabola Technique. Graphite substrates were then irradiated by these ions to fabricate the nanoparticles. The penetration depth of ions into the graphite substrates was measured by using SRIM 2008 software analysis, then the ions implanted samples were etched electrochemically to expose the nanoparticles which were fabricated deeper inside the substrates. The range of the diameter of the nanoparticles fabricated with this method was 40-50 nm. AFM was performed for the surface analysis of the nanoparticles and XRD for the conformation of the particles and for the structural analysis, to analyze the electric conductivity of these nanoparticles these were analyzed by Four-point probe analysis.*

1. INTRODUCTION

Carbide are being defined as the compound composed of carbon and a less electronegative element, so metal carbides are composed of metal and carbon atoms bonded together. Poor metal and transition metal carbides have several unusual properties like greater hardness and very high melting points, metal carbides (MCs) show good mechanical and chemical stability and resistance against corrosion under reaction conditions.. Metal carbides have many application due to their properties, in particular carbides can be used as an effective catalyst for certain chemical reactions that are readily catalyzed by such noble metals as Pt and Pd [1-3], metal carbides are also being used in machine tools and methanol fuel cells [2-4] These materials also show the various catalytic advantages over their parent metals in activity, selectivity, and resistance to poisoning [3]. MCs have been found to be good catalysts for a wide variety of reactions typically catalyzed by noble metals of high cost and limited supply, the similarity of carbides and nitrides to the Group VIII metals was first pointed out by Levy and Boudart [5, 7]. The catalytic properties depend on the surface properties i.e. surface composition, geometric and the electronic properties of the surface; To minimize the amount of metal carbides required for a given level of activity, metal carbides are generally used as metallic carbide nanoparticles which allow larger surface area compared to bulk metallic carbide [6], that is why the nano carbides have attracted the attention of the scientists [3-4]. Here in this paper we are reporting the fabrication of aluminum, tungsten, and copper carbides where aluminum is poor metal while other three are transition metals

2. EXPERIMENTATION

The experimental arrangement was planned in such a way that the energy of ions was found by Thomson Parabola Technique. Nd:YAG laser (1064nm, 9-14 ns, and 10 mJ) was used to irradiate the tungsten target for the production of laser generated ions and graphite was used as a substrate. The higher the energy of incoming ions, the higher will be the penetration depth of the ions into the substrate. Hence after the measurement of energy the penetration depth of ions into the substrate was measured by using SRIM 2008 (Stopping Range of Ions into the Matter) software. These penetrated ions were recombined deeper inside the substrate with the carbon atoms to form the tungsten carbide nanoparticles, and at the last the electrochemical etching was performed to expose the nanoparticles which were fabricated deeper inside the substrate.

The generation of ions depends on different parameters of laser and irradiated material as well. But for a particular laser the production of ions i.e. plasma depends on the threshold value of the material. If the laser intensity is greater than the threshold value of the material then the instantaneous phase transitions take place i.e. heating, melting, boiling and plasma plume production. Once the plasma is produced, it consists of electrons and ions and electrons are lighter particles hence they are more mobile as compare to the ions. Due to the separation of charges the plasma plume stretches, this causes the division of plume into three regions. The first region is region of slow ions and the third region is of faster electrons, whereas the central region is of fast ions and slow electrons. In such a way two regions which are of high potential and low potential are formed which seems to be an electric field for the central region. This field is known as self generated electric field and it causes the forward peaking of ions [8]. The energy of the ions was measured by using the Thomson Parabola Technique [11, 12].

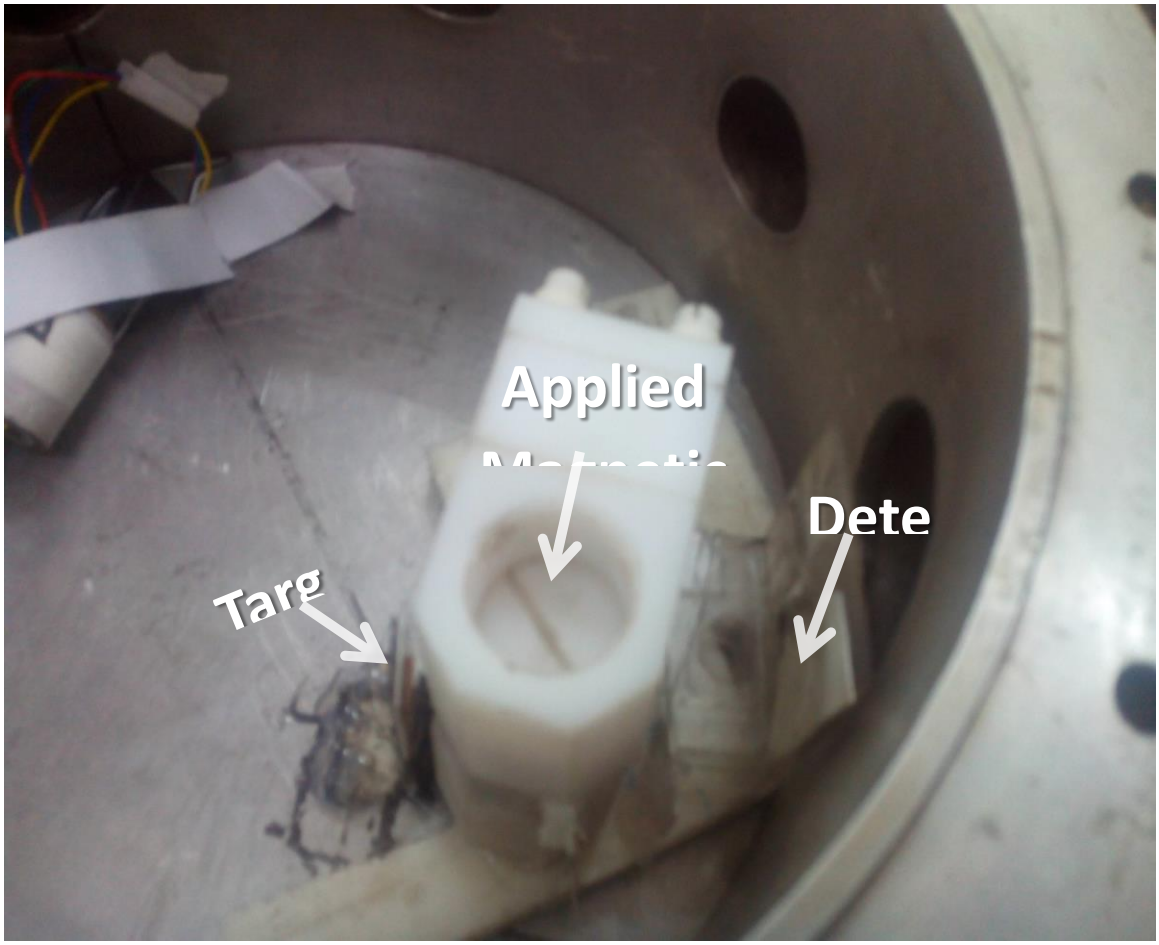

Figure 1: Schematic of Thomson Parabola Technique

Using the Scheme shown in figure 1 the energy of the ions was measured. After measuring the energy the ions, these ions were implanted onto the graphite substrates. The distance between the target and the substrate was taken as 4 cm and sample was implanted for 500 numbers of shots, under medium vacuum. Eight port vacuum chamber was used for this purpose as shown in figure 2.

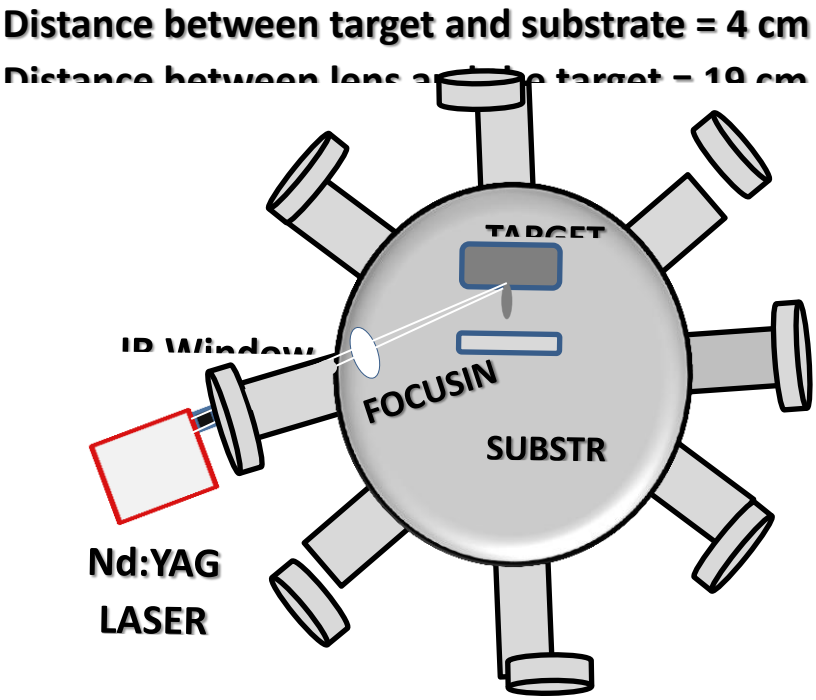

Figure 2: Schematic of ions implantation

After ion implantation the penetration depth of the ions into the substrate was measured using SRIM 2008 software. As these ions were penetrated deeper into the substrate material, after reaching the stopping range of the ions these ions were bonded with the carbon atoms of the inner surface. Hence to expose these carbon-ions bonded atoms (Nanoparticles) we were required to etch the substrate by electrochemical etching.

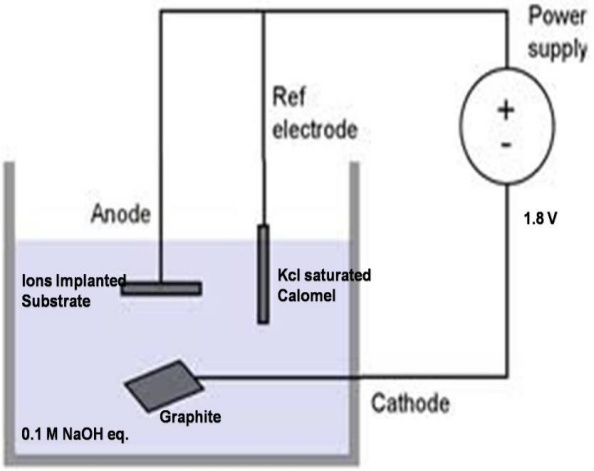

Figure 3: The Schematic of electrochemical etching

Here tungsten ions implanted graphite substrate was used as working electrode, Graphite as counter electrode and the KCl saturated Calomel as a reference electrode. The purpose of reference electrode here is only to maintain the potential difference between the working electrode and the counter electrode. The potential difference between the anode and cathode was 1.8 V, 0.1 molar aqua's solution of NaOH was used as electrolyte in this experiment. This apparatus is called the voltammeter here the reduction and oxidation takes place simultaneously. Reduction takes place at anode and oxidation at cathode, let us discus the chemical changes that take place at anode because we are required etching so we will discuss only the reduction which takes place at anode. Here in case of our experiment the major role is of two phenomena the intercalation and the adsorption [9].

Intercalation is the phenomena in which a molecule sandwiches inside the two layers which are well arranged. When negatively charged hydroxyl ions come to the anode the sandwich themselves between the layers of carbon and bond with them according to the following equation.

$C(s) + OH^- \rightarrow C(s)OH(ads' int) + e^-$

Because the C(s)OH can't remain stable hence it dissolves into the liquid instantly and as a result carbon atom and water produces as shown in the following reaction.

$4C(s)OH(ads' int) \rightarrow 4C + 2H_2O + O_2$

C(s)OH (ads,int) is representing the carbon on the substrate with OH^- chemisorbed or intercalated, while "C" is indicating about the detached carbon atoms. In this way the upper layer of the substrate etches and we are able to expose the nanoparticles. Then these nanoparticles were analyzed by using different kind of experimental techniques for the conformation and structural information of these nanoparticles [9].

3. RESULTS AND DISCUSSION

Thomson parabola technique was used to measure the energy of the ions. CR-39 was used as detector to detect the deflection of ions under the influence of magnetic field. The distance between the detector and the target material was 4.5 cm for all the samples and 0.08 T was the applied magnetic field. The energy of the ions was measured by using equation given as

$$\textbf{Energy} = (e^2B^2R^2)/2M$$

R is the radius of curvature of the deflected path which was measured by applying the relation

$$R = a\,[D/X + \{D^2/X^2 + 1\}^{1/2}]$$

Where a is the diameter of the region were the magnetic field is applied, D is the distance travelled by the ions from magnetic field to the detector and X is the deflection in the path of the charged particles [10, 17]. The value of "a" was taken as 1.5 cm and of "D" was 4.5 throughout the experimentation. To measure the value of X the implanted CR-39 was characterized by optical microscope. The result of Thomson parabola technique for the energy measurement is shown in Table 1.

Table 1: Measurement of Radius of curvature and Energy of the Ions

Ions	Mass (amu)	Value of X (cm)	Value of R (cm)	Value of Energy T(keV)
Tungsten	183.85	0.0543	248.6	10.368

Table 2: SRIM results for measuring the penetration depth of ions into the graphite

Ions	Value of Energy T(keV)	Penetration Depth (Å)
Tungsten	10.368	90-98

After measuring the energy of the ions these ions were implanted into the graphite substrate. The penetration depth of the ions into the graphite was measured by using the SRIM 2008 software the SRIM result is shown in Table 2.

For the conformation of the fabrication of nanoparticles XRD was performed and the size of the particles was confirmed by AFM and at the last the conductivity of the samples was measured by Four Point Probe

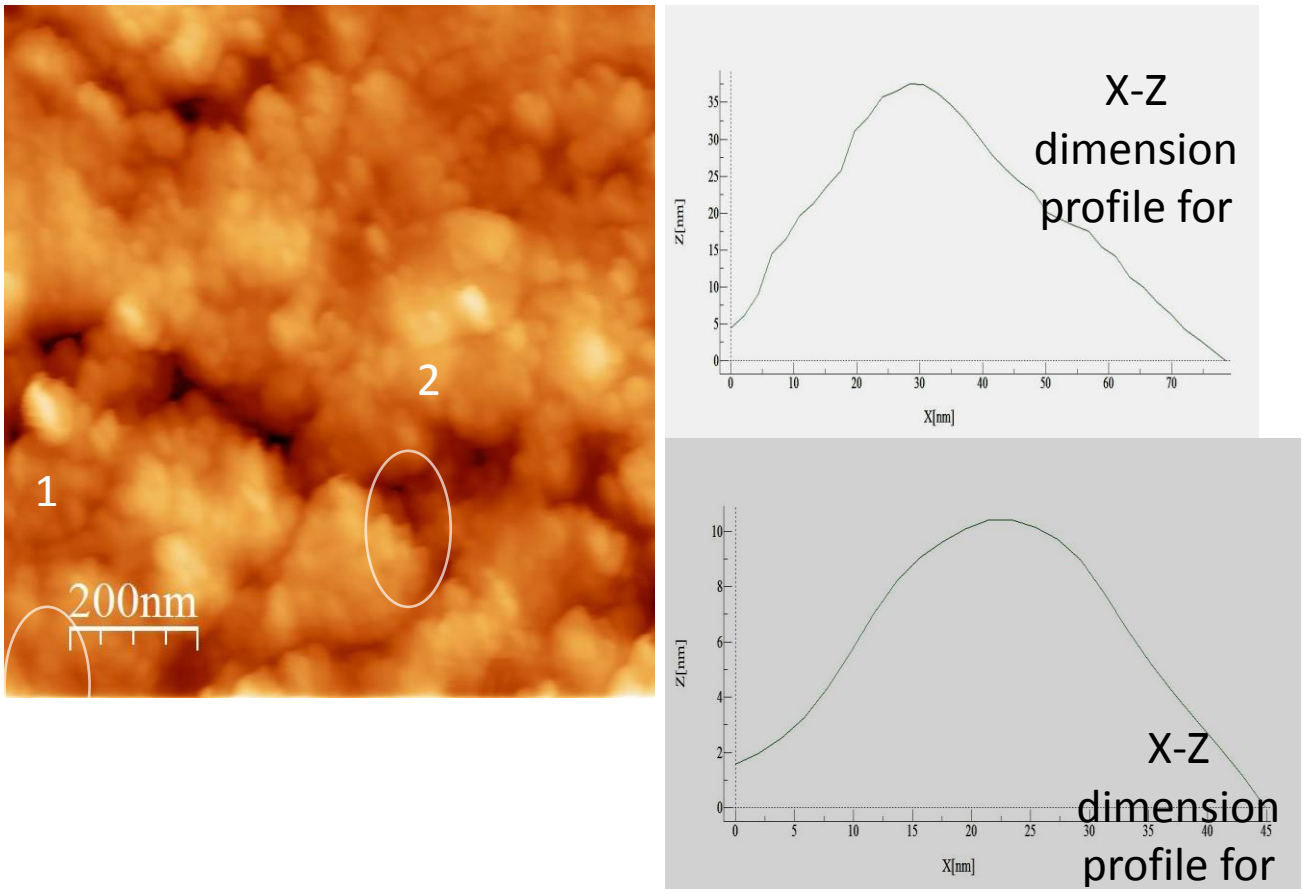

.

Figure 4: (a) AFM Image of Tungsten Carbide nanoparticles (b) Height and diameter profile for different particles

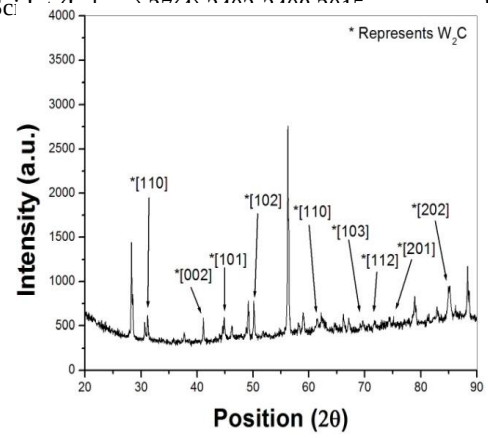

Figure 5: XRD Results of Tungsten Carbide nanoparticles

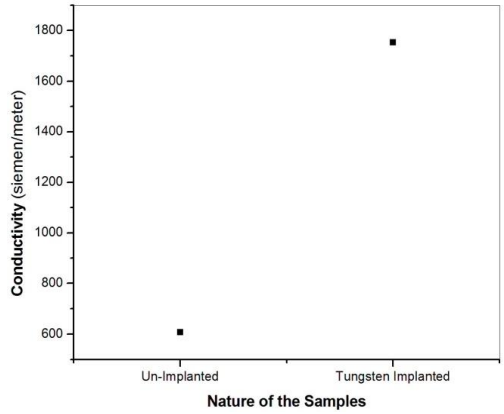

Figure 6: Conductivity of Tungsten Implanted and Un-Implanted Substrates

Figure 4 is clearly showing the successful fabrication of the tungsten carbide nanoparticles, the height and diameter profile of these nanoparticles is also shown in figure from which we can conclude that the tungsten carbide nanoparticles have diameter in the range of ≅ 40-50 nm.

Similarly the structure and nature of tungsten carbide (W_2C) nanoparticles at the graphite substrate was confirmed by XRD, the results of XRD are shown in figure 5. Here nine peaks at positions 34.5241, 38.0295, 39.5695, 52.3, 61.861, 69.7868, 74.9794, 75.9845 and 85.2276 with d-spacing 2.598, 2.36621, 2.27759, 1.74926, 1.49988, 1.34767, 1.2667, 1.25243 and 1.13772 respectively were matching with that of hexagonal tungsten carbide [13-15]. The crystallite size for the copper and tungsten carbide nanoparticles was also measured that was nearly 7.41nm. The XRD results are also presenting the authentication of the AFM results hence the fabrication of carbide nanoparticles was confirmed by the above mentioned XRD and AFM analysis.

The inter-planar distance (d-spacing) and the grain size were measured by using the following equations

$n\lambda = 2d\sin\theta$

$$\text{Grain size (D)} = \frac{0.9\lambda}{\text{FWHM (rad)X } \cos\theta}$$

Where n is order of diffraction, λ is wavelength of X-rays used (For Cu K_α λ ≅ 1.5406 Å),θ is Bragg's angle and d represents the d-spacing [16].

To analyze the electrical properties of these nanoparticles the substrate having these nanoparticles were analyze by Four Point Probe technique. The electrical conductivity was measured by using following formula [20].$\rho = \frac{2\pi sV.CF.}{I}$

Where I = applied current (mA), V = corresponding voltage (nV), S = spacing between the probes = 4 mm (the same for all probes) and CF.= F(w/s) = correction factor = 0.6336 because in our case w/s = 2 where 'w' the thickness of the sample [18]. The electrical conductivity of these nanoparticles was measured by this technique which is shown in figure 9.

The conductivity of the un-implanted substrate and Tungsten Implanted substrate was measures as 608 and 1753 Siemens/meter respectively.

It is observed that for all the specimens, the electrical conductivity increases in a remarkable manner as compare to electrical conductivity of the unexposed sample. The ion beam induced damages on the surface of the material produce defects and stresses in the material that affect on its transport characteristics for electrical conduction. Grain structure of the irradiated alloys are changed due to defects, therefore the electrical conductivity of ions irradiated alloys also changes. Ions irradiation damages on the material surface results in thermal stresses and defects like lattice vacancies and interstitial, points defects, dislocation, grain boundaries, stacking faults, as well as phase boundaries vacancies, clusters, nucleation, voids and spike formation which can cause an increase in electrical conductivity of metals and alloys [19]. At a sufficiently high temperature due to ions implantation and due to the electrochemical etching process as well, recrystallization occurs and produces growth of new strain free and equiaxed grains having low dislocation densities. It is usually accompanied by a decrease in resistivity and increase in conductivity [20].

4. CONCLUSIONS

Tungsten carbide nanoparticles have been fabricated by electrochemical etching of ion implanted graphite substrate. The diameter range of these fabricated nanoparticles was 40-50 nm; which was observed by Atomic Force Microscope, XRD confirmed the presence of tungsten carbide nanoparticles in the substrate. The crystal structure for these nanoparticles was hexagonal. The conductivity of the ions implanted substrates was enhanced due to the excess of free charged particles present in the ion implanted substrate and also due to the change in grain size.

REFERENCES

1) X. G. Yanga! and C. Y. Wang, Nanostructured tungsten carbide catalysts for polymer electrolyte fuel cells, Applied Physics Letters **86**, 224104, (2005).
2) Antonio Luis Tomas-Garcia, Qingfeng Li, Jens Oluf Jensen, Niels J. Bjerrum "High surface area tungsten carbides: synthesis, characterization and catalytic activity towards the hydrogen evolution reaction in phosphoric acid at elevated temperatures" Int. J. Electrochem. Sci., **9**, 1016 – 1032 (2014).

3) Dong Jin Ham and Jae Sung Lee, "Transition metal carbides and nitrides as electrode materials for low temperature fuel cells" Energies, **2**, 873-899, (2009).
4) M. Nakazawa and H. Okamoto "Surface composition of prepared tungsten carbide and its catalytic activity" Applied Surface Science **24**, 75-86, (1985).
5) R.B. Levy, M. Boudart, "Platinum-like behavior of tungsten carbide in surface catalysis" Science 181 547, (1973).
6) E. Fabbri, S. Taylor, A. Rabis, P. Levecque, O. Conrad, R. Kotz, T.J. Schmidt, "The effect of platinum nanoparticle distribution on oxygen electroreduction activity and selectivity" ChemCatChem. **6**, 1410-1418, (2014).
7) S. Ted Oyama, Crystal Structure and Chemical Reactivity of Transition Metal Carbides and Nitrides, Journal of Solid State Chemistry **96**, 442--445 (1992).
8) M. Shahid Rafique, M. Khaleeq ur Rahman, Aziz ul Rehman, Khurram Siraj & M. Fiaz Khan, "Laser produced Copper Ion Energy Spectrum employing Thomson Parabola Technique" Journal Laser Physics, **17**, 3, 282 – 285 (2007).
9) S. Kato, T. Yamaki, S. Yamamoto, T. Hakoda, K. Kawaguchi, T. Kobayashi, A. Suzuki and T. Terai, "Preparation of tungsten carbide nanoparticles by ion implantation and electrochemical etching" Nuclear Instruments and Methods in Physics Research B **314**, 149–152, (2013).
10) L. Reimer, Physics of Image information & Microanalysis, 2nd edition.
11) M. Shahid Rafique, M. Khaleeq ur Rahman, Aziz ul Rehman, Khurram Siraj & M. Fiaz Khan, "Laser produced Copper Ion Energy Spectrum employing Thomson Parabola Technique" Journal Laser Physics (Russia), **17**,3, 282 – 285, (2007).
12) S V Springham, S Lee and M S Rafique," Correlated deuteron energy spectra and neutron yield for a 3 kJ plasma focus" *Plasma Phys. Control. Fusion*, **42**, 1023, (2000).
13) Natl. Bur. Stand. (U.S.) Monogr. **25**, 21, 128, (1984).
14) Metcalfe, A., J. Inst. Met., **73**, 591, (1947).
15) Rudy, E., Windisch, S., J. Am. Ceram. Soc., **50**, 272, (1967).
16) A. Latif, M. Khaleeq-ur-Rahman, K. A. Bhatti, M. S. Rafique, Z. H. Rizvi, 'Crystallography and surface morphology of ion-irradiated silver' **1 6 6**, 4, 265-271 (2011).
17) M. Shahid Rafique, M. Khaleeq-ur-Rahman, Aziz-ul-Rehman, Khurram Siraj, and M. Fiaz Khan, "Laser-Produced Copper Ion Energy Spectrum Employing Thomson Scattering Technique", Laser Physics, **17**, 3, 282–285 (2007).
18) F. M. SMITS, "Measurement of The Sheet Resistivities With Four-Point Probe Manuscript received October 15 (1957).
19) Shazia Bashir, M. S. Rafique, M. Khaleeq-Ur Rahman Faizan ul Haq and B. R. Alvina, "CO2 And Nd:YAG Laser Radition Induced Damage in Aluminum", 15,pp181–192 (2006).
20) Sherif Sedky, "Post-Processing Techniques for Integrated MEMS",Low Thermal Budget Techniques for Enhancing Crystallization" (Artech House, INC, United States of America, 2006).